Journal of Power Sources 267 (2014) 793–798

Contents lists available at ScienceDirect

Journal of Power Sources

journal homepage: www.elsevier.com/locate/jpowsour

Microwave synthesis of an electrocatalyst based on CoFeRu for the oxygen reduction reaction in the absence and presence of methanol

Antonia Sandoval González [a], Francisco Paraguay Delgado [b], Pathiyamattom Joseph Sebastian [c], Edgar Borja Arco [a, *]

[a] Departamento de Física y Química Teórica, Facultad de Química, Universidad Nacional Autónoma de México, Av. Universidad 3000, Ciudad Universitaria D.F. 04510, Mexico
[b] Departamento de Microscopía Electrónica, Centro de Investigación en Materiales Avanzados, Miguel Cervantes 120, CP 31109 Chihuahua, Mexico
[c] Instituto de Energías Renovables, Universidad Nacional Autónoma de México, Privada Xochicalco S/N, Temixco, Mor. 62580, Mexico

HIGHLIGHTS

- CoFeRu catalyst synthesized by a microwave-assisted method.
- Material as ORR catalyst.
- Potential use of this material as DMFC cathode.

ARTICLE INFO

Article history:
Received 12 February 2014
Received in revised form
30 May 2014
Accepted 31 May 2014
Available online 9 June 2014

Keywords:
Microwave
Electrocatalyst
Oxygen reduction reaction
DMFC cathode

ABSTRACT

In this work a simple and rapid synthesis method for obtaining (CoFeRu) based electrocatalyst for the oxygen reduction reaction (ORR) in the absence and presence of methanol is reported. The electrocatalyst is synthesized by microwave thermal heating method in a mixture of ethylene glycol/water as reaction media at 220 °C during 30 min, and 600 W of power radiation. The material is characterized by the rotating disk electrode technique. The electrocatalyst shows tolerance to the presence of 1 mol L^{-1} methanol during the ORR. The material is structurally characterized by X-ray diffraction and its chemical composition is determined by energy-dispersive spectroscopy analysis. The electrocatalyst is a potential candidate to be used as cathode in DMFC.

1. Introduction

Direct methanol fuel cells have been studied for many years. These fuel cells are based on the technology of proton exchange membrane fuel cells and they are good candidates for various applications, mainly in electric vehicles, hospital, and small devices such as laptops, digital cameras and mobile phones [1–3]. However methanol is highly prone to pass through the polymer-electrolyte membrane (cross-over effect). The methanol that comes into contact with the cathode electrocatalyst will reduce the efficiency of the oxygen reduction reaction by a competing electrochemical process.

Typical DMFC anode is carbon-supported platinum electrocatalyst. However sequential stripping of protons and electrons is believed during methanol oxidation, leading to the formation of carbon-containing intermediates, such as linearly bonded-CO_{ads}, and the electrocatalyst become poisoned [4]. The methanol cross-over effect can be reduced using selective cathode electrocatalyst materials [5,6]. In this way, it is necessary to investigate materials that carry on the oxygen reduction reaction with high open circuit potential, catalytic activity and tolerance to the methanol presence. There are many proposals for these electrocatalyst including platinum, Pt alloyed with transition metals or only transition metals [7–11]. Most of the electrocatalysts that show high catalytic activity for ORR are Pt-based [7].

There are few works using Co and Fe as cathodic electrocatalyst by direct methanol fuel cells. For example, Pd–Co/C has been synthesized at different experimental conditions [12,13] and was found that this electrocatalyst shows an excellent ORR activity. Cobalt electrocatalyst has been reported with attractive catalytic activity towards ORR [14,15] and with tolerance toward methanol [16]. The use of iron as cathode in DMFC also has been investigated and was found that the highest catalytic activity was obtained when the iron

* Corresponding author. Tel.: +52 55 56223899.
E-mail addresses: eborjarco@gmail.com, eborja@unam.mx (E. Borja Arco).

http://dx.doi.org/10.1016/j.jpowsour.2014.05.149
0378-7753/

is combined with other metal or when is synthesized at higher temperatures [17–19]. There are many studies with ruthenium electrocatalysts used as cathode in a fuel cell [20–22]. It is found that ruthenium is an excellent candidate as cathode in DMFC [23,24].

The aim of the present work is to study the electrochemical behavior of (CoFeRu)/C electrocatalyst for the oxygen reduction reaction in the absence and presence of methanol. This electrocatalyst is synthesized by microwave thermal heating process.

2. Experimental

2.1. Electrocatalyst synthesis and physical characterization

(CoFeRu) based electrocatalyst is synthesized by microwave thermal heating process [25], using 92 mg of cobalt (II) nitrate hexahydrate ($CoN_2O_6 \cdot 6H_2O$ 99.999%, Sigma–Aldrich), 118 mg of ferrous sulfate heptahydrate ($FeSO_4 \cdot 7H_2O$ 99.9%, Sigma–Aldrich) and 50 mg of triruthenium dodecarbonyl ($Ru_3(CO)_{12}$) 99%, Sigma–Aldrich), dissolved in 7.5 ml of deionized water (18.2 MΩ cm) plus 7.5 ml of ethylene glycol ($HOCH_2CH_2OH$ 99.9%, J.T. BAKER). The mixing is placed in a microwave synthesis reactor (Synthos 3000, Anton Paar), at 220 °C during 30 min. The product is filtered, washed with deionized water/acetone (CH_3CH_3CO 99.6%, Fermont) and dried at room temperature.

(CoFeRu) electrocatalyst is structurally characterized by XRD and EDS. XRD analysis is carried out using a Rigaku DMAX-2200 diffractometer (Cu Kα1 radiation, 1.5406 Å). The X-ray diffraction pattern is obtained using Jade 6.5 software. The chemical composition is investigated by X-ray energy-dispersive spectra (EDS) analysis using a Hitachi SU1510 microscope.

2.2. Electrochemical characterization

The catalytic ink is prepared mixing 0.6 mg of (CoFeRu) electrocatalyst and 1.4 mg of Vulcan XC-72 with 13 μL of a 5% Nafion®/isopropanol solution (ElectroChem) in an ultrasonic bath (Branson 1510) for 5 min. 2 μL of the resulting ink is deposited as a thin layer on the surface of a glassy carbon disk held in a Teflon cylinder of the rotating disk electrode (geometrical surface area was 0.071 cm^2). The layer is dried at room temperature.

The electrochemical studies are carried out at 25 °C, in a conventional three compartment electrolytic cell with a water jacket for maintaining stable temperature conditions in the electrolyte. A mercury sulfate electrode (Hg/Hg_2SO_4/0.5 mol L^{-1} H_2SO_4; abbreviated as MSE) is used as reference electrode (MSE = 0.640V/NHE), which is connected to the cell through a bridge with a lugging capillary. A thick carbon rod is used as counter electrode and 0.5 mol L^{-1} sulfuric acid (H_2SO_4 98%, J.T. Baker) is used as electrolyte. A potentiostat/galvanostat (Solartron Analytical, model SI 1287) and CorrWare™ software are used for the electrochemical measurements and records of experiments.

The electrolyte is purged with nitrogen (Infra; UHP) for the activation of the electrode. This activation is done by scanning (cyclic voltammetry, CV) between 0 and 1.04 V/NHE at 20 mV s^{-1} until no variation on the voltammogram is observed (30 cycles). On the other hand, a Pt/Vulcan-XC-72 (Pt/C) electrode is used for comparison, for which a scanning between 0 and 1.56 V/NHE range is performed, at 50 mV s^{-1} rate. These electrocatalysts has a loading of 1 mg cm^{-2} (geometric area).

Linear sweep voltammetry (LSV) is used for ORR studies [6]. The electrolyte is saturated with pure oxygen (Infra; UHP) for 15 min. Polarization curves in the presence of oxygen ware obtained in the $E_{oc}^{O_2}$ to 0 V/NHE range for the (CoFeRu)/C electrocatalyst at 20 mV s^{-1} and in the $E_{oc}^{O_2}$ to 0.2 V/NHE range for the Pt/C electrocatalyst at 5 mV s^{-1}. Rotation rates ranges from 100 to 1500 rpm.

CV and LSV curves are also obtained in the presence of methanol (1 mol L^{-1} CH_3OH 99.9%, J.T. Baker), under the conditions described above.

3. Results

3.1. Structural composition

Fig. 1 shows the experimental XRD-patterns of the synthesized electrocatalyst. It can be observed that there are not crystallographic peaks well defined for the alloy $Co_xFe_yRu_z$, and different crystalline phases as Ru, Co_3C and $CoFe_2O_4$ are formed, with a crystal size of 9.1, 10.4 and 33.9 nm, respectively. These crystal sizes are in agreement with those reported in the literature [20,26,27].

The chemical composition (At%) of the (CoFeRu) electrocatalyst shows an atomic ratio Co:Fe:Ru of 1.7:1.7:46.6 with a high percentage of carbon (17%) and oxygen (33%). The presence of carbon is due to the carbonyl groups present in $Ru_3(CO)_{12}$ salt, and the oxygen could be attributed at the CoN_2O_6 * $6H_2O$ or $FeSO_4$ * $7H_2O$ salts. With this technique was corroborated that the electrocatalyst shows a higher ruthenium presence (46.6%), which was observed in XRD-patterns.

3.2. Electrochemical characterization

3.2.1. Cyclic voltammetry

Fig. 2 shows the voltammograms of (CoFeRu)/C in the absence and presence of 1 mol L^{-1} methanol solution, along with that for Pt/C for comparison. In the absence of methanol, the (CoFeRu)/C voltammograms (Fig. 2a) shows well-defined peak at established position and the current density value remains constant, indicating that the metal-support bond remains anchored to the surface. These materials show a cathodic peak centered between 0.1 and 0.2 V/NHE similar to that reported for a thin film of ruthenium oxide [28], Ru_2O_3 or $RuO_{2x}H_2O$ [29,30] formed during the anodic sweep. Besides, proton diffusion is also taking place in this potential range [31]. Also is observed the presence of oxygen evolutions peak, in the anodic (0.9–1.1 V/NHE) region. Another important feature is that the (CoFeRu)/C electrocatalyst does not show methanol oxidation peaks, in contrast with the platinum electrode, which exhibits very sharp peaks (Fig. 2b) indicating its high activity for the methanol oxidation process.

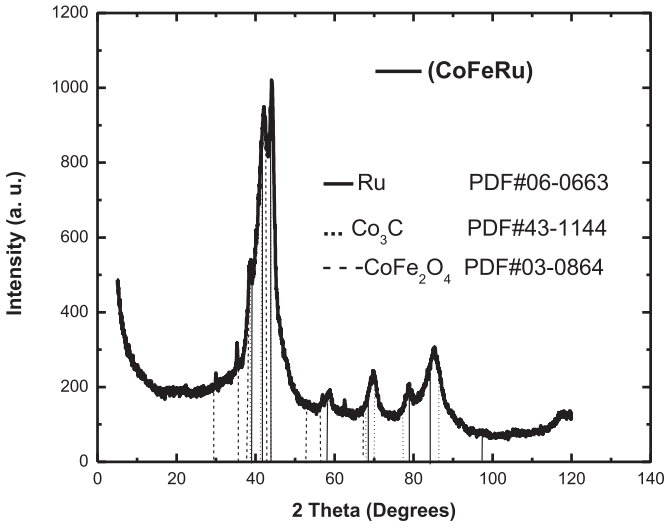

Fig. 1. X-ray diffraction patterns of (CoFeRu) electrocatalyst.

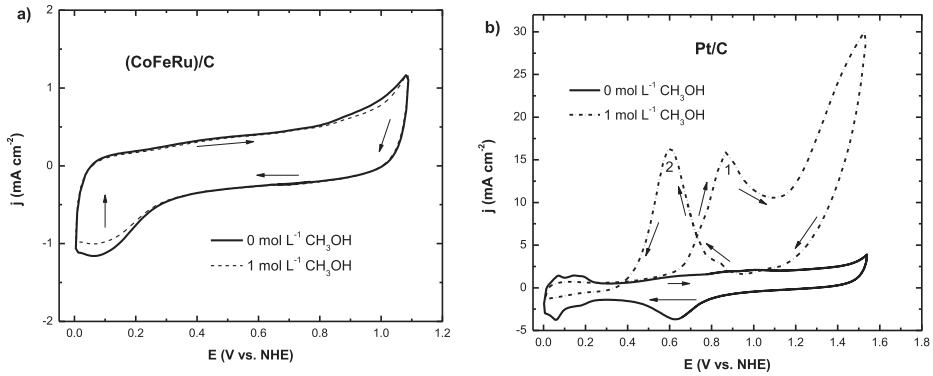

Fig. 2. Cyclic voltammograms in the absence and presence of 1 mol L^{-1} methanol for a) (CoFeRu)/C (sweep rate = 20 mV s^{-1}) and b) Pt/C (the sweep rate = 50 mV s^{-1}). The electrolyte was 0.5 mol L^{-1} H_2SO_4.

3.2.2. Oxygen reduction reaction (ORR)

Fig. 3 shows the polarizations curves of (CoFeRu)/C and Pt/C electrocatalysts for the ORR in the absence and presence of 1 mol L^{-1} CH_3OH solution. These curves show a similar performance in the three distinct regions of the ORR processes in the absence of methanol: 1) the kinetic region, when the current, i_k is independent of the rotation velocity; 2) the mixed control region, where the behavior is determined by kinetic as well as diffusion processes; and 3) the mass transfer region, where the diffusion current, i_d, is a function of the rotation velocity. In the third zone, the transfer of electrons is very fast and the observed process is controlled by the oxygen mass transport diffused at the electrode surface [32].

In the absence of methanol, Pt/C commercial electrocatalyst shows a high activity toward oxygen reduction reaction (Fig. 3a). The open circuit potential begins at 0.87 V/NHE and the current density increase with the increase of the rotation velocity. However, in the presence of methanol the Pt electrode exhibits a net cathodic current onset to shift negatively by ca. 0.3 V/NHE, due to the simultaneous methanol oxidation and oxygen reduction reactions [33]. Moreover, the polarization curves for (CoFeRu)/C electrocatalyst are practically unchanged by the presence of methanol (Fig. 3a), thus confirming the tolerance to methanol during the ORR.

The analysis of the current–potential curves at different rotating rates is carried out by analyzing the hydrodynamic plots in a first order kinetic reaction from a Koutecky–Levich approach [34].

$$\frac{1}{i} = \frac{1}{i_k} + \frac{1}{i_d} \tag{1}$$

where i is the measured disk current, i_k is the current due to the charge-transfer at the electrode surface, and i_d the diffusion controlled current. This equation may be used to separate i_k from i_d, and get the real electrocatalyst activity [35]. For the rotating disk electrode experiment, in the laminar flow regime, the diffusion current is a function of the rotation velocity and hence, Eq. (1) may be written as:

$$\frac{1}{i} = \frac{1}{i_k} + \frac{B}{\omega^{1/2}} \tag{2}$$

ω is the electrode rotation velocity in rpm and B is a constant given by [36]:

$$B = \frac{1}{200nFAC_{O_2}D_{O_2}^{2/3}\nu^{-1/6}} \tag{3}$$

where 200 is a constant used when ω is expressed in revolutions per minute and the current in mA, n is the number of electrons related to the oxygen reduction reaction, A is the geometric area in cm^2, F the Faraday constant (96485C mol^{-1}), C_{O_2} is the oxygen concentration in the bulk of the electrolyte (1.10×10^{-6} mol cm^{-3}), $D_{O_2}^{2/3}$ is the oxygen diffusion coefficient (1.40×10^{-5} cm^2 s^{-1}) and $\nu^{-1/6}$ is the kinematic viscosity of the electrolyte (0.01 cm^2 s^{-1}) [37,38].

The processes involved in the reduction reaction of molecular oxygen at the cathode electrode are much more complex than the hydrogen oxidation processes at the anode electrode. The mechanism for the cathodic oxygen reduction reaction in acid solution involves two overall pathways: the four-electron pathway, where

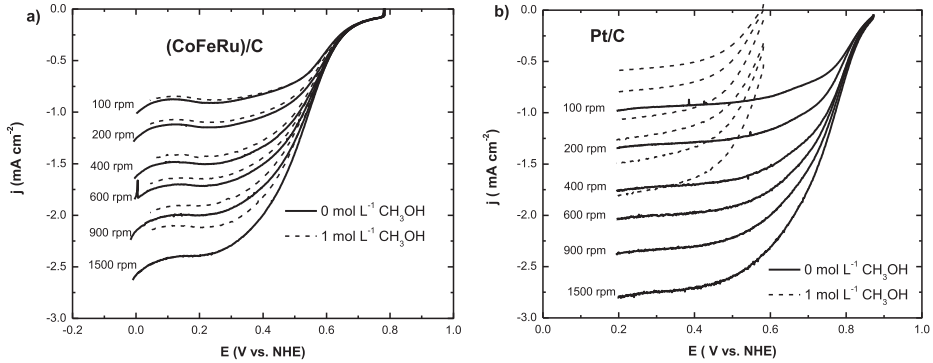

Fig. 3. Steady-state current–potential curves for Oxygen reduction reaction in the absence and presence of 1 mol L^{-1} methanol for a) (CoFeRu)/C and b) Pt/C. The electrolyte was 0.5 mol L^{-1} H_2SO_4 and the sweep rate was 5 mV s^{-1}.

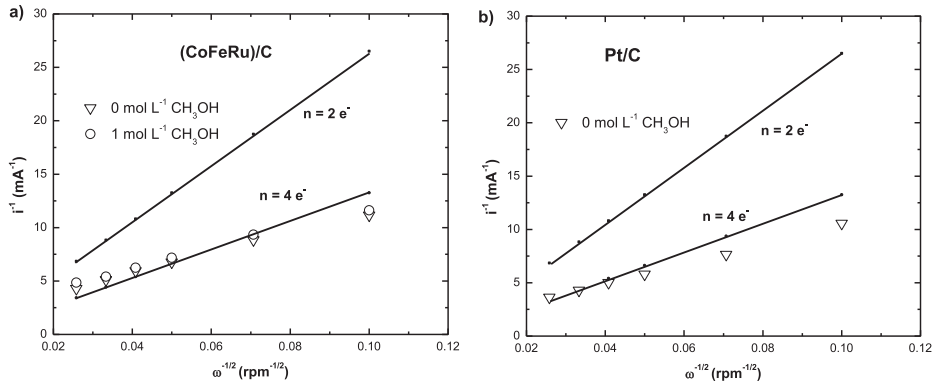

Fig. 4. Experimental (at various potentials) and theoretical (2 and 4 electrons) Koutecky–Levich plots in the absence and presence of 1 mol L^{-1} methanol for a) (CoFeRu)/C and b) Pt/C. Solid lines indicate theoretical four and two electrons for the oxygen reduction mechanism.

molecular oxygen is reduced to H_2O; and the peroxide pathway, where O_2 is reduced to H_2O_2 [32,39–41]. The Koutecky–Levich plots are usually used to estimate the number of electrons involved during the oxygen reduction. Fig. 4 shows the theoretical (with $n = 2$ and $n = 4$; with an electrode geometric area of 0.071 cm^2) and experimental Koutecky–Levich plots in the absence and presence of 1 mol L^{-1} CH_3OH, at a given potential value of 0.4 V/NHE. It can be observed that the Pt/C and (CoFeRu)/C electrocatalysts show a four electron process, indicating that the O_2 is most likely reduced to H_2O, following a direct four electron pathway at the solid electrode/solution interface. The linearity and parallelism of these Koutecky–Levich plots indicate a first-order kinetics with respect to molecular oxygen [42]. The differences between the experimental and theoretical Koutecky–Levich plots may result from the exposed effective surface area (A_{eff}) of the electrocatalyst, which might be higher than the geometric ones [43]. This A_{eff} can be calculated from Eq. (4), using the experimental Koutecky–Levich slope, B_{exp}, and $n = 4$:

$$A_{\text{eff}} = \frac{1}{200nFB_{\text{exp}}C_{O_2}D_{O_2}^{2/3}\nu^{-1/6}} \tag{4}$$

All the current measured are normalized to this effective area. Both electrocatalysts have similar effective surface area values (0.099 cm^2), which are higher than geometric area (0.0701 cm^2). This result is expected because the materials are supported with Vulcan.

Equation (5) can be used to correct for mass transport and thus obtain i_k as a function of potential, Tafel plot [37,44,45].

$$i_{\text{k}} = \frac{i \cdot i_{\text{d}}}{i_{\text{d}-\text{i}}} \tag{5}$$

Fig. 5 shows the mass transport corrected Tafel plots for the oxygen reduction reaction on (CoFeRu)/C and Pt/C, respectively. Table 1 summarizes the effective area (A_{eff}) obtained by experimental Koutecky–Levich slope, the open circuit potential (E_{oc}) and the kinetic parameters obtained from Tafel plots: Tafel slope (b), charge transfer coefficient (α), and the exchange current density (j_0), for the (CoFeRu)/C and commercial Pt/C electrocatalysts.

It can be seen that in the absence and presence of CH_3OH, the $E_{oc}^{O_2}$ values for (CoFeRu)/C electrocatalyst are unaffected by the presence of methanol. Although the Pt/C electrode shows the highest $E_{oc}^{O_2}$ value in the absence of methanol, it shows the lowest value in the presence of methanol, due to the presence of a mixed potential [46].

For the ORR usually two Tafel slopes (b) are obtained, 60 mV dec^{-1} and 120 mV dec^{-1} [30,47], respectively, depending on the electrode materials used and on the potential range. From results presented in Table 1, (CoFeRu)/C shows Tafel slopes higher than commercial platinum. However, Tafel slopes higher than 120 mV dec^{-1} are often observed in reactions through some adsorbed layers at the surface. A thin layer of ruthenium oxide, which exists in the mentioned potential range, could causes an increase in the Tafel slope [29] and the rate-determining step does not correspond to a single electron-transfer, according the following scheme [21]:

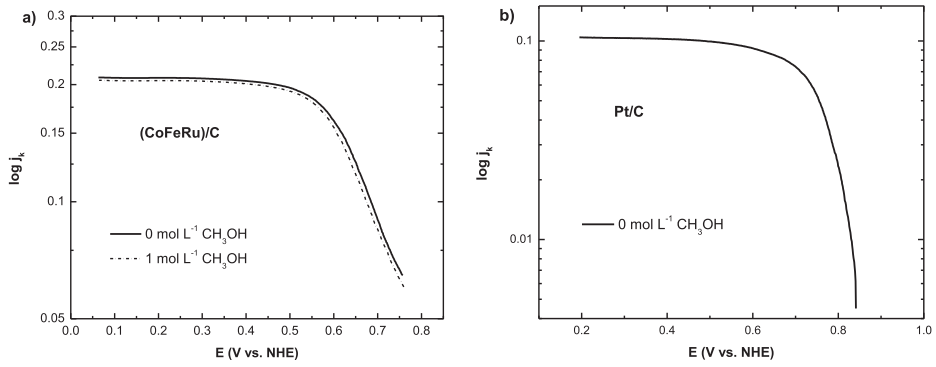

Fig. 5. ORR mass-transfer-corrected Tafel plots in the absence and presence of 1 mol L^{-1} methanol for a) (CoFeRu)/C and b) Pt/C.

Table 1
Effective surface area, open circuit potentials and oxygen reduction reaction kinetic parameters of the (CoFeRu)/C and commercial Pt/C electrocatalysts.

Electrocatalysts	CH_3OH [mol L^{-1}]	A_{eff} cm^2	$E_{oc}^{O_2}$ V vs. NHE	b mV dec^{-1}	α	j_0 mA cm^{-2}
Pt/C	0	0.099	0.870	115	0.510	7.22×10^{-6}
	1	–	0.580	–	–	–
Ru_x [20]	0	–	0.800	110	0.53	4.29×10^{-6}
	1	–	–	–	–	–
(CoFeRu)/C	0	0.098	0.782	193	0.306	2.49×10^{-4}
	1	0.098	0.780	203	0.306	3.20×10^{-4}

$$O_2 + H^+ + e^- \rightarrow O_2H \quad (6)$$

The charge transfer coefficient (α) is a parameter that has been related with the free energy of activation for a reduction process [48]. The (CoFeRu)/C electrocatalyst shows similar α (0.306) values in the absence and presence of 1 mol L^{-1} CH_3OH, which means that this material spends the same energy for, begins the reaction in the absence and presence of CH_3OH. Commercial platinum electrocatalyst shows the highest α value in the absence of methanol, but in methanol presence it can not be calculated due to the reaction competition of oxygen reduction reaction and methanol oxidation reaction.

Exchange current density (j_0) is an important kinetic parameter representing the electrochemical reaction rate at equilibrium [48]. The magnitude of the j_0 determines how rapidly the electrochemical reaction can occur. The j_0 of an electrochemical reaction depends on the reaction and on the electrode surface on which the electrochemical reaction occurs. j_0 is also related to the true electrode area and to the reactant concentration (or partial pressure, for a gas) [32] and it is proportional to the rate constant (k) of the reaction (ORR). In general, the (CoFeRu)/C electrocatalyst shows a higher j_0 than commercial platinum electrocatalyst, as expected from their higher Tafel slopes.

In summary, it was possible to synthesize a material with a high electroactivity toward ORR in the absence and presence of methanol, with a microwave irradiation method avoiding long synthesis periods (>5 h) for the synthesis of this kind of materials.

4. Conclusions

In this work, (CoFeRu)/C electrocatalyst is easily prepared by a microwave thermal heating process. From XRD and EDS results, it is found that electrocatalyst shows different phases with a lower amount of Co (atomic ratio, 1.7%) and Fe (1.7%), and a higher amount of Ru (atomic ratio, 46.6%). The (CoFeRu)/C electrocatalyst shows a high activity for oxygen reduction reaction. In addition, this material shows tolerance to the presence of CH_3OH during the ORR, in contrast to platinum. The microwave method reduces the long times used in the conventional thermolysis processes using for the synthesis of this kind of materials.

Acknowledgments

The authors wish to thank DGAPA-UNAM by the Antonia Sandoval González postdoctoral grant. This work was supported by project PAPIIT-IA102113-UNAM, project PAIP-5000-9014-UNAM and project Conacyt-UNAM 123122 (LiFYCS) for using SEM/EDS Hitachi SU1510. We would like to thank Maria Luisa Ramón and José Campos for valuable technical assistance.

References

[1] H. Razmi, E. Habibi, H. Heidari, Electrochim. Acta 53 (2008) 8178–8185.
[2] S. Siracusano, A. Stassi, V. Baglio, A.S. Aricó, F. Capitanio, A.C. Tavares, Electrochim. Acta 54 (2009) 4844–4850.
[3] A. Sandoval-González, E. Borja-Arco, Jaime Escalante, O. Jiménez-Sandoval, S.A. Gamboa, Int. J. Hydrogen Energy 37 (2012) 1752–1759.
[4] F. Ye, J. Li, T. Wang, Y. Liu, H. Wei, J. Li, X. Wang, J. Phys. Chem. C 112 (2008) 12894–12898.
[5] S.S. Dipti, U.C. Chung, J.P. Kim, W.S. Chung, Phys. Stat. Sol.(a) 204 (2007) 4174–4177.
[6] C. Jeyabharathi, P. Venkateshkumar, J. Mathiyarasu, K.L.N. Phani, Electrochim. Acta 54 (2008) 448–454.
[7] M.H. Lee, J.S. Do, J. Power Sources 188 (2009) 353–358.
[8] K. Lee, L. Zhang, H. Lui, R. Hui, Z. Shi, J. Zhang, Electrochim. Acta 54 (2009) 4704–4711.
[9] M.A. García-Contreras, S.M. Fernández-Valverde, J.R. Vargas-García, M.A. Cortés-Jácome, J.A. Toledo-Antonio, C. Ángeles-Chavez, Int. J. Hydrogen Energy 33 (2008) 6672–6680.
[10] J.J. Salvador-Pascual, S. Citalán-Cigarroa, O. Solorza-Feria, J. Power Sources 172 (2007) 229–234.
[11] Z.-Q. Liu, Q.-Z. Xu, J.-Y. Wang, N. Li, S.-H. Guo, Y.-Z. Su, H.-J. Wang, J.-H. Zhang, S. Chen, Int. J. Hydrogen Energy 38 (2013) 6657–6662.
[12] Y.-C. Wei, C.-W. Liu, Y.-W. Chang, C.-M. Lai, P.-Y. Lim, L.-D. Tsai, K.-E. Wang, Int. J. Hydrogen Energy 35 (2010) 1864–1871.
[13] W.E. Mustain, J. Prakash, J. Power Sources 170 (2007) 28–37.
[14] M. Wang, H. Zhang, H. Zhong, Y. Ma, Int. J. Hydrogen Energy 36 (2011) 720–724.
[15] S. Ye, A.K. Vijh, Int. J. Hydrogen Energy 30 (2005) 1011–1015.
[16] L. Wang, L. Zhang, L. Bai, L. Han, S. Dong, Electrochem. Commun. 34 (2013) 68–72.
[17] V. Bambagioni, C. Bianchini, J. Filippi, A. Lavacchi, W. Oberhauser, A. Marchionni, S. Moneti, F. Vizza, R. Psaro, V. Dal Santo, A. Gallo, S. Recchia, L. Sordelli, J. Power Sources 196 (2011) 2519–2529.
[18] M. Neergar, V. Gunasekar, R. Rahul, J. Electroanal. Chem. 658 (2011) 25–32.
[19] L. Zhang, J. Kim, E. Dy, S. Ban, K.-C. Tsay, H. Kawai, Z. Shi, J. Zhang, Electrochim. Acta 108 (2013) 480–485.
[20] R.G. González-Huerta, J.A. Chávez-Carvayar, O. Solorza-Feria, J. Power Sources 153 (2006) 11–17.
[21] A. Altamirano-Gutiérrez, O. Jiménez-Sandoval, J. Uribe-Godínez, R.H. Castellanos, E. Borja-Arco, J.M. Olivares-Ramírez, Int. J. Hydrogen Energy 34 (2009) 7983–7994.
[22] J.-H. Choi, C.M. Johnston, D. Cao, P.K. Babu, P. Zelenay, J. Electroanal. Chem. 662 (2011) 267–273.
[23] K. Suárez-Alcántara, O. Solorza-Feria, J. Power Sources 192 (2009) 165–169.
[24] S.P. Chiao, D.-S. Tsai, D.P. Wilkinson, Y.-M. Chen, Y.-S. Huang, Int. J. Hydrogen Energy 35 (2010) 6508–6517.
[25] A. de La Hoz, A. Díaz-Ortiz, A. Moreno, Microwaves in Organic Synthesis, second ed., Wiley-VCH, Weinheim, 2006, pp. 219–277.
[26] P. Gao, Y. Wang, S. Yang, Y. Chen, Z. Xue, L. Wang, G. Li, Y. Sun, Int. J. Hydrogen Energy 37 (2012) 17126–17130.
[27] S.R. Ahmed, S.B. Ogale, G.C. Papaefthymiou, R. Ramaesh, P. Kofinas, Appl. Phys. Lett. 80 (2002) 1616–1618.
[28] S. Hadži-Jordanov, H. Angerstein-Kozlowska, M. Vukovlć, B.E. Conway, J. Phys. Chem. B 81 (1977) 2271–2279.
[29] M. Metikoš-Huković, R. Babić, F. Jović, Z. Grubač, Electrochim. Acta 51 (2006) 1157–1164.
[30] M. Vuković, D. Ćukman, J. Electroanal. Chem. 474 (1999) 167–173.
[31] W. Sugimoto, H. Iwata, K. Yokoshima, Y. Murakami, Y. Takasu, J. Phys. Chem. B 109 (2005) 7330–7338.
[32] A.J. Bard, L.R. Faulkner, Electrochemical Methods, Fundamentals and Applications, second ed., John Wiley & Sons, New York, 2001.
[33] K. Lee, O. Savadogo, A. Ishihara, S. Mitsushima, N. Kamiya, K.-I. Ota, J. Electrochem. Soc. 153 (2006) A20–A24.
[34] S. Treimer, A. Tang, D.C. Johnson, Electroanalysis 14 (2002) 165–171.
[35] V.Y. Filinovsky, Y.V. Pleskov, Rotating Disk and Ring-disk Electrodes, Plenum, New York, 1984.
[36] E. Gileadi, Electrode Kinetics, VCH Publishers, New York, 1993, p. 839.
[37] E. Borja-Arco, R.H. Castellanos, J. Uribe-Godínez, A. Altamirano-Gutiérrez, O. Jiménez-Sandoval, J. Power Sources 188 (2009) 387–396.
[38] N. Alonso-Vante, H. Tributsch, O. Solorza-Feria, Electrochim. Acta 40 (1995) 567–576.
[39] J.O.'M. Bockris, A.K.N. Reddy, Modern Electrochemistry, vol. 1, Plenum Publishing Corporation, New York, 1977.
[40] C.M. Sánchez-Sánchez, J. Bard, Anal. Chem. 81 (2009) 8094–8100.
[41] X. Li, Principles of Fuel Cells, Taylor & Francis Group, New York, 2006.
[42] K. Suárez-Alcántara, A. Rodríguez-Castellanos, R. Dante, O. Solorza Feria, J. Power Sources 157 (2006) 114–120.
[43] R.G. González-Huerta, R. González-Cruz, S. Citalán-Cigarroa, C. Montero-Ocampo, J. Chavez-Carvayar, O. Solorza-Feria, J. New. Mater. Electrochem. Syst. 8 (2005) 15–23.
[44] J.L. Gojković, S.K. Zečević, R.F. Savinell, J. Electrochem. Soc. 145 (11) (1998) 3713–3720.

[45] K. Kinoshita, Electrochemical Oxygen Technology, John Wiley & Sons, New York, 1992.
[46] M.R. Tarasevich, G.V. zhutaeva, V.A. Bogdanovska, M.V. Radina, M.R. Ehrenburg, A.E. Chalykh, Electrochim. Acta 52 (2007) 5108–5118.
[47] E. Borja-Arco, O. Jiménez-Sandoval, J. Escalante-García, A. Sandoval-González, P.J. Sebastian, Int. J. Hydrogen Energy 36 (2011) 103–110.
[48] C. Song, J. Zhang (Eds.), PEM Fuel Cell Electrocatalysts and Catalyst Layers Fundamentals and Applications, Springer, Vancouver, 2008, pp. 89–134.